



Structural phase transition and high temperature phase structure of Friedels salt, $3\text{CaO} \cdot \text{Al}_2\text{O}_3 \cdot \text{CaCl}_2 \cdot 10\text{H}_2\text{O}$

G. Renaudin^a, F. Kubel^b, J.-P. Rivera^c, M. Francois^{a,*}

^aLaboratoire de Chimie du Solide Minéral, UMR 7555, Université Henri Poincaré, Nancy I, F-54506 Vandoeuvre les Nancy, France

^bInstitut für Mineralogie, Kristallographie und Strukturchemie Technische Universität Wien, Getreidemarkt 9, A-1060 Wien, Austria

^cDépartement de Chimie Minérale, Analytique et Appliquée Université de Genève, 30 quai Ernest Ansermet, CH-1211 Genève 4, Switzerland

Received 16 March 1999; accepted 10 September 1999

Abstract

Friedels salt, the chlorinated compound $3\text{CaO} \cdot \text{Al}_2\text{O}_3 \cdot \text{CaCl}_2 \cdot 10\text{H}_2\text{O}$ (AFm phase), presents a structural phase transition at about 30°C from a monoclinic to a rhombohedral phase. It has been studied by X-ray powder diffraction and optical microscopy in transmitted light with crossed polarisers on single crystals prepared by hydrothermal synthesis. The high temperature phase was determined at 37°C from X-ray single crystal diffraction data. The compound crystallises in the space group $R\bar{3}c$ with lattice parameters of $a = 5.7358(6)\text{Å}$ and $c = 46.849(9)\text{Å}$ ($Z = 3$ and $D_x = 2.111\text{ g/cm}^3$). The refinement of 498 independent reflections with $I > 2\sigma(I)$ led to a residual factor of 7.1%. The Friedels salt can be described as a layered structure with positively charged main layers of composition $[\text{Ca}_2\text{Al}(\text{OH})_6]^+$ and negatively charged layers of composition $[\text{Cl}^- \cdot 2\text{H}_2\text{O}]$. The chloride anions are surrounded by 10 hydrogen atoms, of which six belong to hydroxyl groups and four to water molecules. The structural phase transition may be related to the size of the chloride anions, which are not adapted to the octahedral cavity formed by bonded water molecules. © 2000 Elsevier Science Ltd. All rights reserved.

Keywords: Crystal structure; X-ray diffraction; Chloride; Friedels salt; Structural transition

1. Introduction

Friedels salt is the common name of the chlorinated lamellar double hydroxide (LDH) of composition $3\text{CaO} \cdot \text{Al}_2\text{O}_3 \cdot \text{CaCl}_2 \cdot 10\text{H}_2\text{O}$. This compound was mentioned for the first time by Friedel in 1897 [1], who studied the reactivity of lime with aluminium chloride. The hydrated tetracalcium bichloroaluminate belongs to AFm phases and is part of a family of hydrated compounds found in cement pastes. The sample appears as platelike hexagonal crystals.

The room temperature structure was determined from single crystals by Terzis and al. [2]; in this paper, the existence of a high temperature (above 30°C) modification was determined. The low temperature (at room temperature) modification crystallises in the monoclinic space group $C2/c$ with $V = 906.64(9)\text{Å}^3$, $a = 9.979(3)\text{Å}$, $b = 5.751(2)\text{Å}$, $c = 16.320(6)\text{Å}$, and $\alpha = 104.53(3)^\circ$. The structure is formed of positively charged rigid main layers (composition $[\text{Ca}_2\text{Al}(\text{OH})_6]^+$) separated by layers of composition $[\text{Hal}^- \cdot$

$y\text{H}_2\text{O}]$, where Hal^- is Cl^- and $y = 2$ in the case of Friedels salt. Nevertheless, the given description of the structure leaves some unanswered questions. For the crystallographic site of the chloride, the indicated Wyckoff 4(e2) site, which is necessary to assure the stoichiometry, is incompatible with the coordinates (1/4, -0.42451 , 1/4) given in the paper.

This paper presents the study of the structural phase transition from X-ray powder diffraction data and from observations using an optical microscope in transmitted light. The high temperature modification of the Friedels salt was determined from X-ray single crystal diffraction intensities measured at elevated temperature (37°C).

2. Methods

2.1. Sample preparation

Crystalline samples with the composition of $3\text{CaO} \cdot \text{Al}_2\text{O}_3 \cdot \text{CaCl}_2 \cdot 10\text{H}_2\text{O}$ were prepared by hydrothermal synthesis as described in our previous works on the monocarboaluminate $3\text{CaO} \cdot \text{Al}_2\text{O}_3 \cdot \text{CaCO}_3 \cdot 11\text{H}_2\text{O}$ [3,4] and bintrialuminate $3\text{CaO} \cdot \text{Al}_2\text{O}_3 \cdot \text{Ca}(\text{NO}_3)_2 \cdot 10\text{H}_2\text{O}$ [5]. The starting powder is a homogeneous mixture of $\text{Ca}(\text{OH})_2$, $\text{Al}(\text{OH})_3$, and $\text{CaCl}_2 \cdot 6\text{H}_2\text{O}$ (Prolabo products) in molar ratio of 3/2/1.

* Corresponding author. Tel.: +33-3-83-91-24-99; fax: +33-3-83-91-21-66.

E-mail address: framcos@lcm.u-nancy.fr (M. Francois)

The resulting phases were examined by X-ray powder diffraction (XRPD). The composition of selected single crystals was checked by using a scanning electronic microscope (SEM) equipped with an energy-dispersive spectrometer (EDS).

2.2. Optical microscope in transmitted light

A Leitz Orthoplan-Pol optical microscope type with an objective 10×/ 0.30 and an 10× ocular was used (Leitz, Wetzlar, Switzerland). The observed single crystal was studied in polarised light. A photographic device (Photo-automat MPS 55 Leica, Heerbrugg, Switzerland) was employed. To study the phase transition, single crystals (both immersed or not immersed in optical oil) were progressively heated by a hot stream air.

2.3. X-ray diffraction

XRPD was performed on a multidetector INEL CPS 120 diffractometer (INEL, Ardenay, France) equipped with a high temperature system. The sample was introduced in a Lindeman tube to avoid preferred orientation problems. Data were recorded in transmission between 0 and 115° degrees in 2θ at 0, 10, 20, 30, and 40°C using monochromated [Quartz α (101)] CuKα1 radiation ($\lambda = 1.54056\text{Å}$) and a counting time of 10,800 s for each pattern.

One selected single crystal was then mounted on an automatic CAD-4 Nonius diffractometer (NONIUS, Delft, The Netherlands). To perform a data collection of the high temperature modification of Friedels salt, the chosen temperature was adjusted at $37 \pm 1^\circ\text{C}$ (i.e., just above the transition). A low cost heating device [6] was used.

Data collection and refinement parameters are summarised in Table 1. The lattice parameters are refined with CAD-4 software [7] from 25 reflections in the θ range 6 to 13°. They are in agreement with the unit cell proposed by Fischer et al. [8] (i.e. $a = 5.7422(5)\text{Å}$ and $c = 46.847(7)\text{Å}$).

The data reduction, in Laue group $\bar{3}m$, was performed using programs of Blessing's system [9]. Absorption corrections were made using the ABSORB program [9], leading to average equivalent reflections with a reliability factor $R(\text{int})$ of 0.042. The structure was then resolved by direct methods with SIR97 program [10] in the space groups $R\bar{3}c$ and $R3c$. Scattering factors used for structure factors calculation and Fourier transformed analysis were those of neutral atoms H, O, Al, Cl, and Ca. These values were taken from International Tables for Crystallography [11]. The structure was finally refined in the centrosymmetric $R\bar{3}c$ space group by least squares method using the SHELX97 program package [12]. The refinement of 27 parameters, using three restraints, leads to a final confidence factor $R1$ of 0.071 for 498 reflections [$I > 2\sigma(I)$]. Restraints with a standard deviation have been applied on H atoms position: distance O-H = $0.95(1)\text{Å}$, distance O(w)-H(w) = $0.95(1)\text{Å}$, and angle H(w)-O(w)-H(w) = $104.5(1.0)^\circ$. All non-H-atoms were refined with anisotropic displacement parameters. For

Table 1

Crystal data and structure refinement for high temperature modification of Friedels salt

Compound	Friedels salt at 37°C ($3\text{CaO} \cdot \text{Al}_2\text{O}_3 \cdot \text{CaCl}_2 \cdot 10\text{H}_2\text{O}$)
Formula weight	561.34 g · mol ⁻¹
Temperature	310(1) K
Wavelength	0.56050 Å
Scan mode	w-2θ
Crystal system	Rhombohedral
Space group	$R\bar{3}c$
Unit cell	
dimensions	$a = 5.724(2)\text{Å}$, $c = 46.689(5)\text{Å}$
Volume	$1324.8(7)\text{Å}^3$
Z/calculated	
density	$3/2.111\text{ g} \cdot \text{cm}^{-3}$
Absorption	
coefficient	0.866 mm^{-1}
$F(000)$	864
Crystal size	$0.200 \times 0.140 \times 0.035\text{ mm}^3$
Theta range for	
data collection	2.06° at 29.93°
Index ranges	$0 \leq h \leq 8$, $0 \leq k \leq 8$, $0 \leq l \leq 82$
Reflections collected/	
independent	2734/746 [$R(\text{int}) = 0.042$]
Refinement method	Full-matrix least-squares on F^2
Number of data/	
restraints/	
parameters	498 [$I > 2\sigma(I)$]/3/27
Goodness-of-fit on F^2	1.130
Final R indices	
[$I > 2\sigma(I)$]	$R1 = 0.0712$, $wR2 = 0.1092$
Largest difference	
peak and hole	$0.530\text{ e} \cdot \text{Å}^{-3}$ and $-0.718\text{ e} \cdot \text{Å}^{-3}$

H atoms the temperature factors were fixed to $1.20 U_{eq}$ of the corresponding O atom.

3. Results and discussion

3.1. Structural phase transition study

3.1.1. XRPD

Selected 2θ ranges of XRD powder patterns are presented as a function of the temperature (by heating from 0 to 40°C) in Fig. 1.

In the first approach, the broadening of the lowest angle reflection and a displacement from $2\theta = 11.24^\circ$ (indexed as 002 in the low temperature lattice) to $2\theta = 11.33^\circ$ (indexed as 006 in high temperature lattice) can be observed when the sample was heated from 0 to 40°C. Thus, a slight decrease of layers spacing (from 7.87Å to 7.81Å) occurs during the structural phase transition.

Second, the powder pattern at 30°C changed significantly, with new Bragg's peaks appearing. Thus the powder pattern can be interpreted as being a mixing of the low and high temperature phases, meaning that the transition is not complete at that temperature.

Finally, at 40°C, the powder pattern presents fewer Bragg peaks and corresponds to the pure high temperature phase. Thus, at 40°C the structure of the Friedels salt is

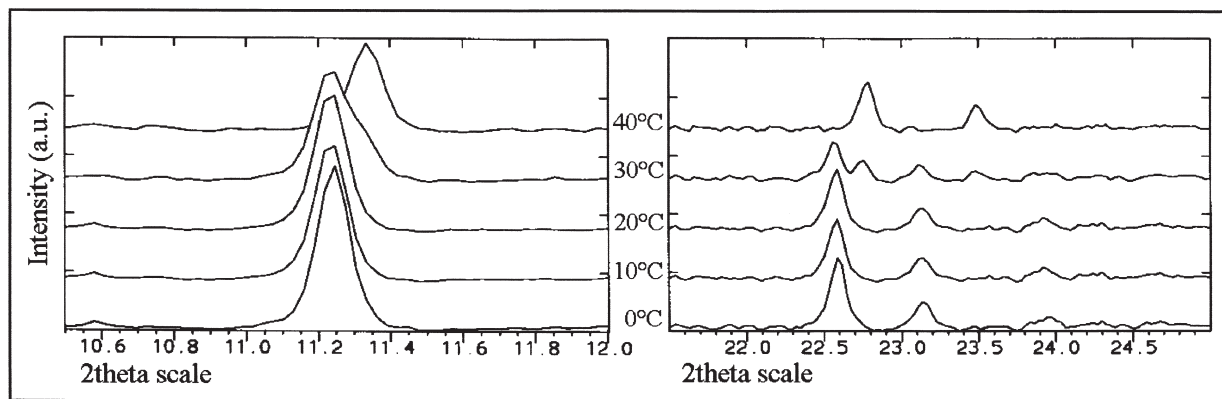


Fig. 1. Selected 2θ ranges of XRD powder patterns of Friedels salt between 0 and 40°C [$\lambda(\text{CuK}\alpha 1) = 1.54056 \text{ \AA}$].

completely transformed. Bragg peaks situated between 2θ range 0 to 60° (not shown here) can be indexed in the hexagonal setting of the rhombohedral group ($R\bar{3}c$) with $a = 5.7358(6)\text{\AA}$ and $c = 46.849(9)\text{\AA}$. The observed and calculated data are given in Table 2. This result is in agreement with the unit cell given by Fischer et al. [8].

Comparison of the monoclinic (at room temperature [2]) and hexagonal lattices show a decreasing of the unit cell volume of 2.6% when changing from the room temperature to the high temperature phase.

3.1.2. Optical microscopy

Fig. 2 was obtained as a series realised with a burst chronological succession of photos (from photo a to f) and shows the structural phase transition of a polydomain crystal of Friedels salt. The crystal has a hexagonal plate shape with the crystal face (0001) perpendicular to the plate. The structural phase transition from a monoclinic to the rhombohedral symmetry leads to a change of the optical properties. The monoclinic modification is biaxial, thus anisotropic and birefringent. The ferroelastic domains appears coloured in polarised light (photo a taken at room temperature); the

rhombohedral high temperature modification is uniaxial with the optical axis parallel to c , so it appears isotropic and transparent (as seen on photo f). This behaviour is in agreement with hexagonal symmetry of the high temperature phase, the hexagonal \bar{c} axis being parallel to the polarised light beam. During the first-order phase transition, the walls of the various domains are moving and then finally disappear. The final state is a single domain crystal of the high temperature phase (photo f).

The transition is quasi-instantaneous and reversible. A better observation of the reversible phase transition is possible when the crystal is immersed in optic oil. This observation allows the further conclusion that the indicated phase transition is not due to a loss of water (dehydration), because of the hydrophobic character of oil, but is a displacive transition, without change of composition.

The observation of a thermal hysteresis indicates a first-order transition. The measured transition temperature on heating was $34.2(3)^\circ\text{C}$ and on cooling $32.0(5)^\circ\text{C}$ (with a heating rate of $\pm 2^\circ\text{C}/\text{min}$). The displacement of the domain walls during the structural phase transition are well defined. And it was possible by stopping heating to keep the crystal with some low temperature domains and a high temperature domain, simultaneously.

The polydomain crystals of the low temperature modification are not suitable for structural resolution. Synchrotron powder diffraction data might improve the resolution and could allow an accurate structural analysis by the Rietveld method. The optical analysis showed that monodomain crystals can be easily obtained by heating just above 30°C ; the latter are well adapted for XRD analysis.

3.2. Structural resolution of high temperature phase

Atomic parameters are reported in Tables 3 and 4 and selected interatomic distances are given in Table 5.

A polyhedral representation of the structure is given in Fig. 3. Description of the main layer $[\text{Ca}_2\text{Al}(\text{OH})_6]^+$ is the usual one undertaken for other AFm phases [2–5,13]. The interlayer has the composition $[\text{2H}_2\text{O}, \text{Cl}^-]$. The coordina-

Table 2

Calculated (calc.) and observed (obs.) Bragg position from high temperature phase of Friedels salt at 40°C ($\lambda_{\text{CuK}\alpha 1} = 1.54056\text{\AA}$) and calculated relative intensities I/I_0 from structural parameters of Table 3

Index	$2\theta_{\text{obs.}}$	$2\theta_{\text{calc.}}$	I/I_0	Index	$2\theta_{\text{obs.}}$	$2\theta_{\text{calc.}}$	I/I_0
0 0 6	11.331	11.323	100	0 2 10	41.099	41.101	18
0 0 12	22.767	22.759	20	0 1 20	42.650	42.640	11
0 1 8	23.501	23.465	34	2 0 14	45.443	45.441	2
1 0 10	26.108	26.125	6	0 0 24	46.437	46.484	2
1 1 0	31.160	31.161	21	1 1 18	47.111	47.115	<1
1 1 3	31.694	31.696	2	0 2 16	48.009	47.995	<1
1 1 6	33.266	33.254	3	2 0 17	49.102	49.105	11
0 0 18	34.459	34.430	8	1 2 8	51.020	51.044	4
1 1 9	35.712	35.716	1	2 1 10	52.475	52.464	3
2 0 2	36.355	36.346	8	2 0 20	53.765	53.748	18
0 2 4	36.961	36.968	6	2 1 13	55.105	55.113	<1
1 1 12	38.925	38.936	4	0 3 0	55.437	55.449	17
2 0 8	39.382	39.375	15	3 0 6	56.802	56.792	2

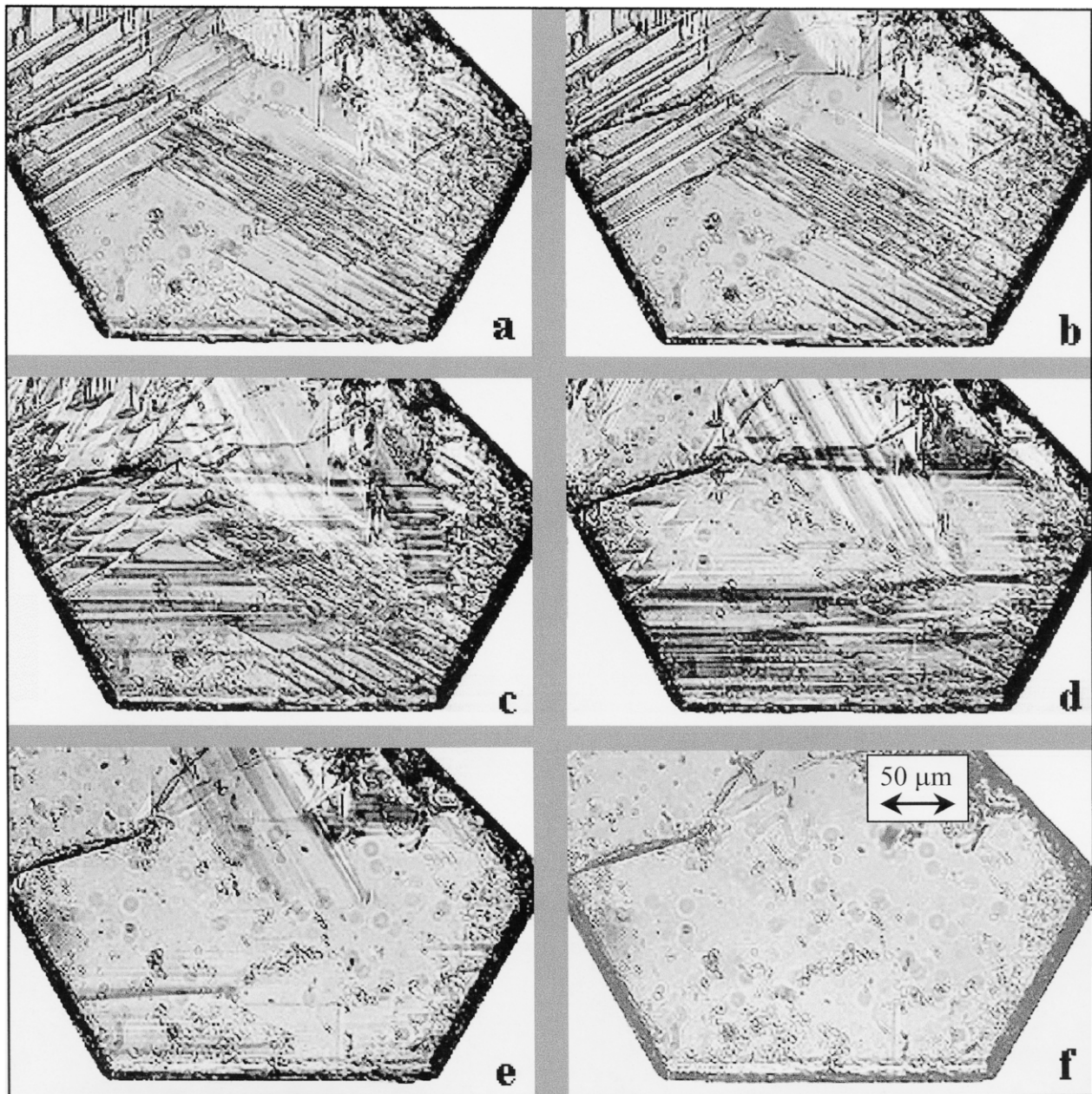


Fig. 2. The structural phase transition was observed by optical microscopy in transmitted polarised light (burst of photos taken during one transition). (a) Birefringent polydomain single crystal (low temperature phase); (b–e) Displacement of the domain walls during the structural phase transition; (f) A transparent single domain crystal (high temperature phase).

Table 3

Atomic coordinates and equivalent isotropic displacement parameters ($\text{\AA}^2 \times 10^3$) for high temperature phase of Friedels salt

Groups	Atoms	Sites	x	y	z	U_{eq}^a ($\text{\AA}^2 \times 10^3$)	Occupancy
	Al	6(b)	0	0	0	14(1)	1
	Ca	12(c)	2/3	1/3	0.9873(1)	16(1)	1
Hydroxyl	O	36(f)	0.0569(4)	0.3071(4)	-0.0213(1)	16(1)	1
	H	36(f)	0.143(6)	0.335(7)	-0.0391(4)	20(-)	1
Water	O(w)	12(c)	2/3	1/3	0.9340(1)	54(1)	1
	H(w)	36(f)	0.57(2)	0.158(2)	0.9261(7)	65(-)	2/3
Chloride	Cl	6(a)	0	0	1/4	67(1)	1

U_{eq} is defined as one third of the trace of the orthogonalized U_{ij} tensor.

Table 4
Anisotropic displacement parameters ($\text{\AA}^2 \times 10^3$) for high temperature phase of Friedels salt

Atoms	U_{11}	U_{22}	U_{33}	U_{23}	U_{13}	U_{12}
Al	10(1)	10(1)	22(1)	0	0	5(1)
Ca	11(1)	11(1)	26(1)	0	0	6(1)
O	15(2)	13(1)	22(2)	2(1)	3(1)	8(1)
O(w)	64(2)	64(2)	35(2)	0	0	32(1)
Cl	86(2)	86(2)	31(1)	0	0	43(1)

The anisotropic displacement factor exponent takes the form:
 $-2\pi^2(h^2a^2U_{11} + \dots + 2hka^*b^*U_{12})$.

tion numbers of the Al^{3+} and Ca^{2+} ions are six and seven, respectively. Each Ca^{2+} is approached by an O(w) atom of a water molecule. From the composition of the main layer and the interlayer, it appears that all water molecules present in the interlayer region of the structure are directly bonded to the main layers via Ca atoms. So Friedels salt does not contain any space filling water in contrast to the carbonated [3,4], nitrated [5], or sulphated [13] equivalent compounds.

The Cl atoms, fully ordered on 6(a) site in the interlayer, are situated at the midway of two adjacent main layers. Chloride atoms are placed in an octahedral cavity formed by O(w) positions, and are directly bonded to H atoms via hydrogen bonds to hydroxyl groups and water molecules. Cl atoms are surrounded by 10 hydrogen atoms on average. Six H atoms at a distance of 2.644Å belong to hydroxyl groups (three from two adjacent main layers) and four H(w) atoms at a distance of 2.478Å belong to water molecules with O(w) atoms ordered on 12(c) site and H(w) atoms distributed on 36(f) general position with an occupancy factor of

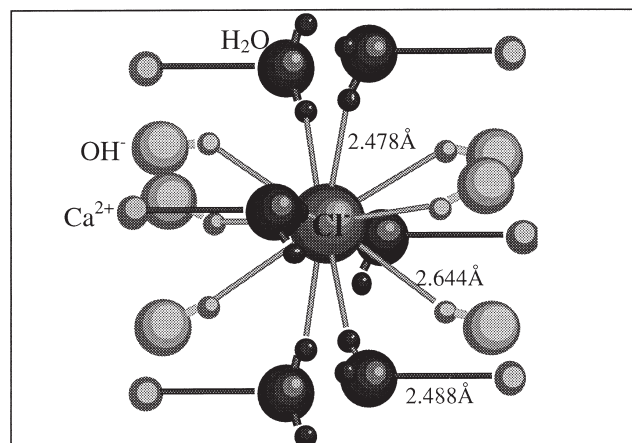


Fig. 4. Hydrogen environment of chloride anion: six H atoms from hydroxyl groups at 2.644Å and six H atoms (at maximum) at 2.478Å from water molecules, which are bonded to Ca^{2+} cation.

2/3. Fig. 4 shows more clearly the environment of chloride anions. Cohesion of the structure between the main layer and interlayers is ensured by hydrogen bonds network, and is mainly between chlorine ions and water molecules following the sequence $\text{Ca} \cdots \text{O}(\text{w})\text{-H}(\text{w}) \cdots \text{Cl} \cdots \text{H}(\text{w})\text{-O}(\text{w}) \cdots \text{Ca}$.

The assumption can be made that at room temperature the size of Cl^- atoms is too small to fill the octahedral cavity formed by water molecules. Preliminary results are in progress to study equivalent compounds containing Br^- and I^- ions. For these compounds the structural phase transition temperature correlates with ionic size. The monoclinic distortion that results from a displacement of the main layers

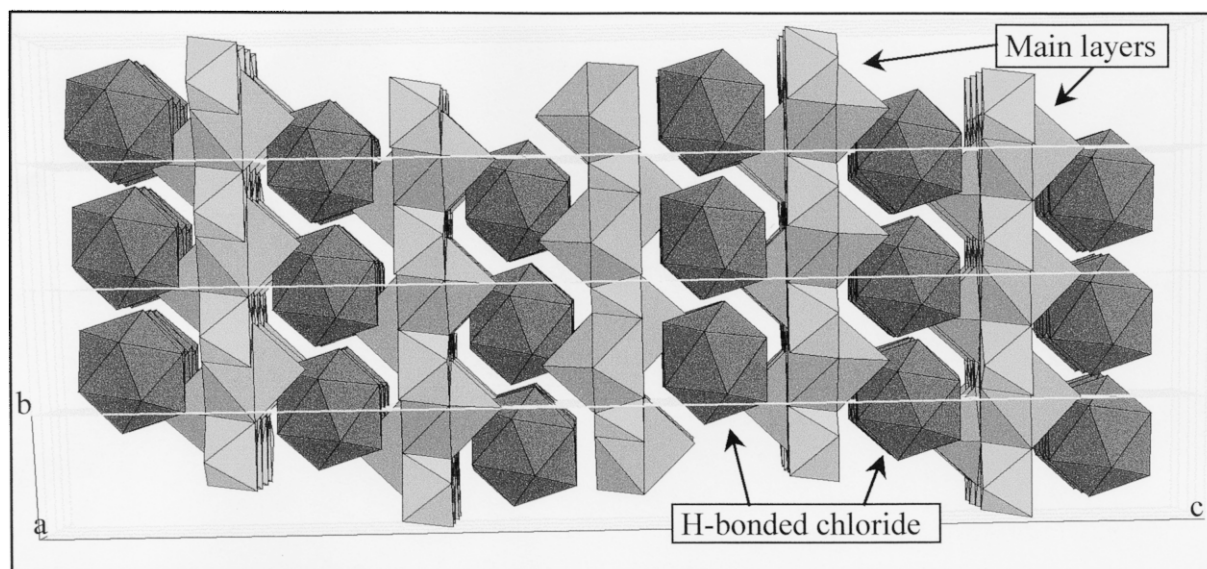


Fig. 3. Perspective polyhedral representation of high temperature structure of Friedels salt, projection along [100] direction. Al and Ca are in oxygen six and seven coordination, respectively. Cl atoms are represented in hydrogen 12 maximum coordination, despite the fact that coordination of Cl atoms is 10 on average (see text).

Table 5
Selected interatomic distances Ca-O, Al-O, and Cl-H of Friedels salt of the high temperature modification

Atoms	Distance (Å)
Al-O	$6 \times 1.900(2)$
Ca-O	$3 \times 2.237(2)$
	$3 \times 2.449(2)$
-O(w)	$2 \times 2.488(5)$
Four distances, on average	
Cl-H(w)	2.478(2)
Cl-H	$6 \times 2.644(2)$

allows the four water molecules connected to them to approach the central Cl^- anion. Above 30°C , the distortion is not necessary as thermal agitation of chlorine atoms may be sufficient to fill these cavities. It releases the stacking constraints, leading to a displacement of the layers coherent with a higher symmetry.

4. Conclusions

These studies confirm clearly, by means of optical microscopy and XRPD, that the structural phase transition of Friedels salt occurs above 30°C , which was first discovered by Terzis et al. [2]. The transition is of the displacive type. The structural parameters of the high temperature modification have been determined for the first time. They indicate that the origin of the transition may be due to the size of Cl atoms, which is not well suited to the dimension of the interlayer site formed by water molecules. The structural phase transition from monoclinic to a rhombohedral structure leads to a decrease of the interlayer spacing and of the volume.

A structural study of the low temperature Friedels salt phase using powder XRD pattern would be useful to validate these explications. Further, the influence of the halogen atom on the structural phase transition is being studied.

Acknowledgments

The authors are grateful to the Service Commun de Diffractométrie Automatique of the University Henri Poincaré in Nancy, and to Alain Rouillier from the Laboratoire d'Expérimentation Haute Température—Basse Pression (CRPG), Nancy, for the autoclave manipulations.

References

- [1] P.M. Friedel, Sur un chloro-aluminate de calcium hydraté se maclant par compression, *Bull Soc Franç Minéral* 19 (1897) 122–136.
- [2] A. Terzis, S. Filippakis, H.J. Kuzel, H. Burzlaff, The crystal structure of $\text{Ca}_2\text{Al}(\text{OH})_6\text{Cl}\cdot 2\text{H}_2\text{O}$, *Zeit Krist* 181 (1987) 29–34.
- [3] M. François, G. Renaudin, O. Evrard, A cementitious compound with composition $3\text{CaO} \cdot \text{Al}_2\text{O}_3 \cdot \text{CaCO}_3 \cdot 11\text{H}_2\text{O}$, *Acta Cryst C* 54 (1998) 1214–1217.
- [4] G. Renaudin, M. François, O. Evrard, Order and disorder in the lamellar hydrated tetracalcium monocarboaluminate compound, *Cem Concr Res* 29 (1999) 63–69.
- [5] G. Renaudin, M. François, The lamellar double-hydroxide (LDH) compound with composition $3\text{CaO} \cdot \text{Al}_2\text{O}_3 \cdot \text{Ca}(\text{NO}_3)_2 \cdot 10\text{H}_2\text{O}$, *Acta Cryst C* 55 (1999) 835–838.
- [6] O. Crottaz, F. Kubel, H. Schmid, High temperature single crystal X-ray diffraction: Structure of cubic manganese iodine and manganese bromine boracite, *J Solid State Chem* 120 (1) (1995) 60–65.
- [7] Enraf-Nonius, CAD-4 software version 5.0, Enraf-Nonius, Delft, The Netherlands, 1989.
- [8] R. Fischer, H.J. Kuzel, H. Schellhorn, Hydrocalumit: Mischkristalle von Friedelschem Salz $3\text{CaO} \cdot \text{Al}_2\text{O}_3 \cdot 10\text{H}_2\text{O}$ und tetracalciumaluminat-hydrat $3\text{CaO} \cdot \text{Al}_2\text{O}_3 \cdot \text{Ca}(\text{OH})_2 \cdot 10\text{H}_2\text{O}$, *Neues Jahrb Mineral Monatsch* H7 (1980) 322–334.
- [9] R.H. Blessing, Data reduction and error analysis for accurate single crystal diffraction intensities, *Crystallogr Rev* 1 (1987) 3–58.
- [10] A. Altomare, M.C. Burla, M. Camalli, G. Cascarano, C. Giacovazzo, A. Guagliardi, G. Polidori, SIR97 program: A new tool for crystal structure determination, *J Appl Cryst* 32 (1999) 115–119.
- [11] International Tables for Crystallography, Volume C, A.J.C. Wilson (Ed.), Kluwer Academic Publishers, Dordrecht, 1992.
- [12] G.M. Sheldrick, SHELX97, Program for the refinement of crystal structure, University of Göttingen, Germany, 1997.
- [13] R. Allmann, Refinement of the hybrid layer structure $[\text{Ca}_2\text{Al}(\text{OH})_6]^+ [1/2\text{SO}_4 \cdot 3\text{H}_2\text{O}]^-$, *Neues Jahrb Mineral Monatsch* H3 (1977) 136–143.